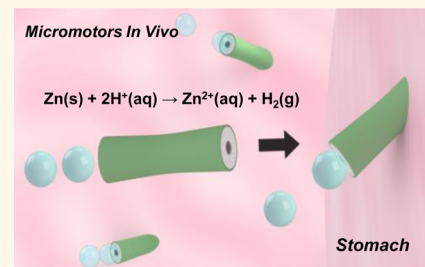


Artificial Micromotors in the Mouse's Stomach: A Step toward *in Vivo* Use of Synthetic Motors

Wei Gao,[†] Renfeng Dong,[†] Soracha Thamphiwatana,[†] Jinxing Li, Weiwei Gao, Liangfang Zhang,^{*} and Joseph Wang^{*}

Department of Nanoengineering, University of California, San Diego, La Jolla, California 92093, United States. [†]W.G., R.D., and S.T. contributed equally.

ABSTRACT Artificial micromotors, operating on locally supplied fuels and performing complex tasks, offer great potential for diverse biomedical applications, including autonomous delivery and release of therapeutic payloads and cell manipulation. Various types of synthetic motors, utilizing different propulsion mechanisms, have been fabricated to operate in biological matrices. However, the performance of these man-made motors has been tested exclusively under *in vitro* conditions (outside the body); their behavior and functionalities in an *in vivo* environment (inside the body) remain unknown. Herein, we report an *in vivo* study of artificial micromotors in a living organism using a mouse model. Such *in vivo* evaluation examines the distribution, retention, cargo delivery, and acute toxicity profile of synthetic motors in mouse stomach via oral administration. Using zinc-based micromotors as a model, we demonstrate that the acid-driven propulsion in the stomach effectively enhances the binding and retention of the motors as well as of cargo payloads on the stomach wall. The body of the motors gradually dissolves in the gastric acid, autonomously releasing their carried payloads, leaving nothing toxic behind. This work is anticipated to significantly advance the emerging field of nano/micromotors and to open the door to *in vivo* evaluation and clinical applications of these synthetic motors.



KEYWORDS: nanomotors · zinc · *in vivo* · cargo delivery · toxicity

The development of small-scale synthetic motors that convert energy into movement and forces has been a fascinating research area.^{1–8} Impressive progress made over the past decade has led to a variety of powerful microscale motors based on different propulsion mechanisms and design principles. New functionalities and capabilities have been added to these micromotors, leading to advanced microscale machines that offer a wide range of important applications. In particular, the movement of man-made micromachines in biological fluids can benefit biomedical fields such as directed drug delivery, diagnostics, nanosurgery, and biopsy.^{9–13} For example, functional micromotors have shown considerable promise for isolating circulating tumor cells and bacteria from raw biological fluids.^{14,15} Mallouk et al. have recently reported the ultrasound-driven propulsion of nanowire motors in living cells,¹⁶ while Nelson et al. have explored targeted drug delivery based on magnetically propelled artificial flagella.¹⁷ *In vitro*

testing by Pumera's team found no apparent toxicity effects of catalytic microengines on cell viability.¹⁸ Although tremendous progress has been made toward such biomedical applications,^{9–13} there are no reports so far illustrating and examining the *in vivo* operation and behavior of these tiny micromotors. Lacking the characterization and evaluation of these synthetic motors in whole living organisms greatly hinders their further development toward practical and routine biomedical applications.

Here we demonstrate the first study of synthetic motors under *in vivo* conditions, involving acid-powered zinc-based micromotors in a living organism. Among the variety of recently developed artificial micromotors, our recently reported zinc-based motors hold great promise for *in vivo* use, particularly for gastric drug delivery, because of their unique features, including acid-powered propulsion, high loading capacity, autonomous release of payloads, and nontoxic self-destruction.^{19,20} Fabricated through established membrane templating

* E-mail: josephwang@ucsd.edu.
* E-mail: zhang@ucsd.edu.

Received for review December 12, 2014
and accepted December 30, 2014.

Published online December 30, 2014
10.1021/nn507097k

© 2014 American Chemical Society

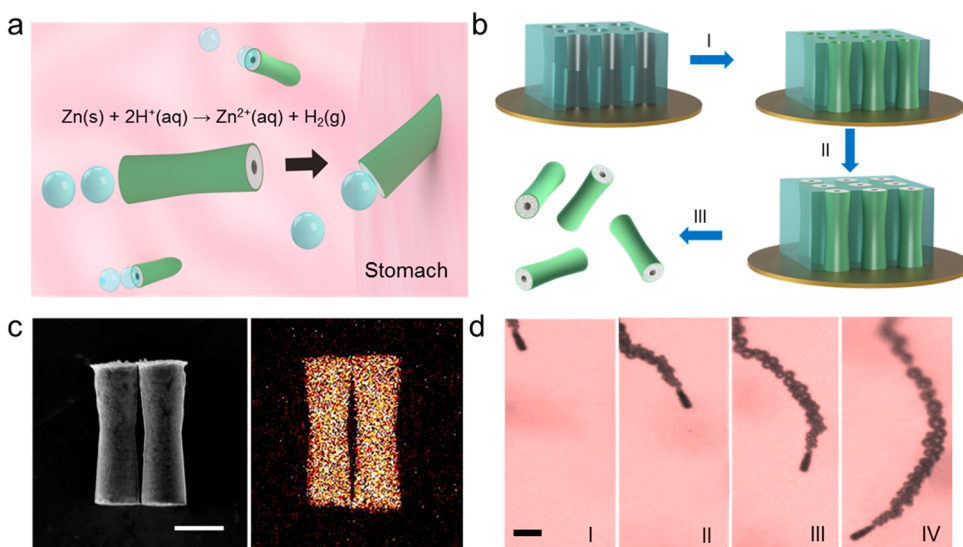


Figure 1. Preparation and characterization of PEDOT/Zn micromotors. (a) Schematic of the *in vivo* propulsion and tissue penetration of the zinc-based micromotors in mouse stomach. (b) Preparation of PEDOT/Zn micromotors using polycarbonate membrane templates: (I) deposition of the PEDOT microtube, (II) deposition of the inner zinc layer, and (III) dissolution of the membrane and release of the micromotors. (c) Scanning electron microscopy (SEM) image (left) of the PEDOT/Zn micromotors and the corresponding energy-dispersive X-ray spectroscopy (EDX) data (right) of elemental Zn in the micromotors. Scale bar, 5 μm. (d) Time lapse images (1 s intervals, I–IV) of the propulsion of PEDOT/Zn micromotors in gastric acid under physiological temperature (37 °C). Scale bar, 20 μm.

processes, the zinc-based micromotors can display efficient propulsion in a harsh acidic environment without additional fuel and transport fully loaded cargoes at high speeds. As the zinc body is dissolved by the acid fuel, the motors are self-destroyed, leaving no harmful chemicals behind.^{19,20} Such attractive behavior makes these zinc-based micromotors useful for movement and operation in the harsh stomach environment, hence opening the door to the first *in vivo* operation of micro/nanomotors in living animals.

In this study, the zinc-based micromotors are applied to the stomach of living mice through gavage administration. The autonomous movement of these motors in gastric acid and the motion-induced biodistribution and retention of the micromotors on the stomach wall are carefully evaluated, along with their *in vivo* toxicity profile. Our results demonstrate that the self-propulsion of the micromotors leads to a dramatically improved retention of their payloads in the stomach lining compared to the common passive diffusion and dispersion of orally administrated payloads. These findings, along with the absence of toxic effects in stomach, indicate that the movement of micromotors in the stomach fluid offers potentially distinct advantages for *in vivo* biomedical applications and pave the way for their future clinical studies.

RESULTS AND DISCUSSION

Figure 1a illustrates the self-propulsion and tissue penetration of acid-driven poly(3,4-ethylenedioxythiophene)(PEDOT)/zinc(Zn) micromotors in the stomach environment. The PEDOT/Zn bilayer micromotors were fabricated using Cyclopore polycarbonate membrane

templates containing microconical pores (Figure 1b). Due to solvophobic and electrostatic effects, the monomers initially polymerized on the inner wall of the membrane pores, leading to a rapid formation of the outer PEDOT layer.²¹ A zinc layer was subsequently deposited galvanostatically within the PEDOT microtube. The resulting PEDOT/Zn bilayer microstructures were then released by dissolving the membrane templates. Figure 1c (left) displays a side-view SEM image of two typical PEDOT/Zn micromotors. Such biconical micromotors have a length of 20 μm and a diameter of 5 μm. Energy-dispersive X-ray mapping analysis, carried out to confirm the motor composition (Figure 1c, right), illustrates the presence of zinc throughout the motor body. Immersion of the PEDOT/Zn micromotors in the gastric acid resulted in a spontaneous redox reaction involving the Zn oxidation and the generation of hydrogen bubbles essential for the propulsion thrust. Figure 1d displays time-lapse images, taken from the Supporting Information video S1, for the movement of the PEDOT/Zn micromotor in a simulated gastric acid (pH 1.2) over a 3 s period at 1 s intervals (I–IV). These images illustrate a defined tail of hydrogen microbubbles generated on the inner Zn surface and released from one side of the micromotors, propelling the micromotors at a high speed of ~60 μm/s. Such efficient propulsion of the zinc-based micromotors at the gastric pH indicates considerable promise for *in vivo* evaluation and operation, as envisioned in Figure 1a.

In order to demonstrate that the zinc-based micromotors hold such distinct advantages for *in vivo* operation and potential for biomedical applications, we first

examined their retention properties on the stomach tissues using a mouse model. The micromotors were administered to the mice orally after the mice were fasted overnight (in order to avoid the influence of food). To examine the effect of the micromotor propulsion upon the tissue penetration, we compared the retention behavior of PEDOT/Zn micromotors with that of PEDOT/Pt micromotors (which cannot move in the stomach environment and thus serve as a control). Following 2 h of the micromotors administration, the mice were sacrificed and their entire stomach was excised and opened. Subsequently, the luminal lining was rinsed with PBS and flattened for imaging and micromotors counting. The gastric tissue obtained from the mice treated with PEDOT/Zn micromotors displayed a large amount of micromotors retained on the stomach lining 2 h post-administration (Figure 2a). In contrast, a significantly smaller amount of the control PEDOT/Pt micromotors (which are very stable in the stomach environment and do not exhibit autonomous propulsion) was retained on the stomach wall using the same experimental conditions (Figure 2d). Apparently, the propulsion of the Zn-based micromotors in the acidic stomach environment greatly improved their tissue penetration and retention. It is well

documented that the inner surface of the stomach is covered by a 170 μm thick mucus layer, which is composed primarily of cross-linked and entangled mucin fibers.²² When the conical motors are actively propelled in the stomach, they have a great chance to penetrate into the porous, gel-like mucus layer and be trapped within the mucus. The retention of PEDOT/Zn micromotors in the gastric tissue was further examined at 6 and 12 h after their administration (Figure 2b,c). The number of micromotors retained in the stomach tissues decreased gradually from 285 per mm^2 to 70 per mm^2 and to 25 per mm^2 at 2, 6, and 12 h post-oral administration, respectively (Figure 2e). Such a time-dependent decrease of motor retention in the mouse stomach is likely due to further degradation of the anchored motors under gastric conditions as well as their transfer to the subsequent digestive systems such as the small intestine. Nevertheless, the results clearly demonstrate that even after 12 h micromotors are still observed in the stomach tissue, indicating the efficient tissue penetration of the motors.

Next, we tested the *in vivo* functionalities of such PEDOT/Zn micromotors for possible applications, particularly for cargo delivery in living organisms. In our previous study,²⁰ we reported the *in vitro* capabilities of Zn-based micromotors for combinational cargo delivery and multifunctional operation, including autonomous release of cargo and self-destruction of the motors during the acid-driven movement of the zinc motors. Taking advantage of these attractive capabilities, we demonstrated here that PEDOT/Zn micromotors could effectively deliver the cargoes *in vivo*. Compared to the previously reported fully loaded zinc micromotors that could operate only in an extremely strong acid and had very short lifetimes (<1 min),²⁰ the presence of the outer PEDOT polymeric layer here greatly enhances the propulsion performance and lifetime of the zinc micromotors under a broad spectrum of acidic conditions characteristic of the stomach environment. Such PEDOT based micromotors can be self-propelled for ~10 min in the stomach environment under physiological temperature (pH up to 2). In this study, gold nanoparticles (AuNPs) were employed as a model cargo because of their widespread use as imaging agents and drug carriers.²³ Figure 3a (left) shows an SEM image of a PEDOT/Zn micromotors loaded with AuNPs (~50 nm diameter) through vacuum infiltration before the zinc deposition. The corresponding EDX mapping analysis indicates a uniform distribution of elemental Zn and Au over the entire micromotor body (Figure 3a, center and right panel, respectively), which confirms the successful encapsulation of the AuNP cargoes. Note that the AuNPs are hardly observed in the SEM image because of their extremely small size and confinement within the Zn body. Supporting Information video S2 displays the autonomous propulsion of two AuNPs loaded

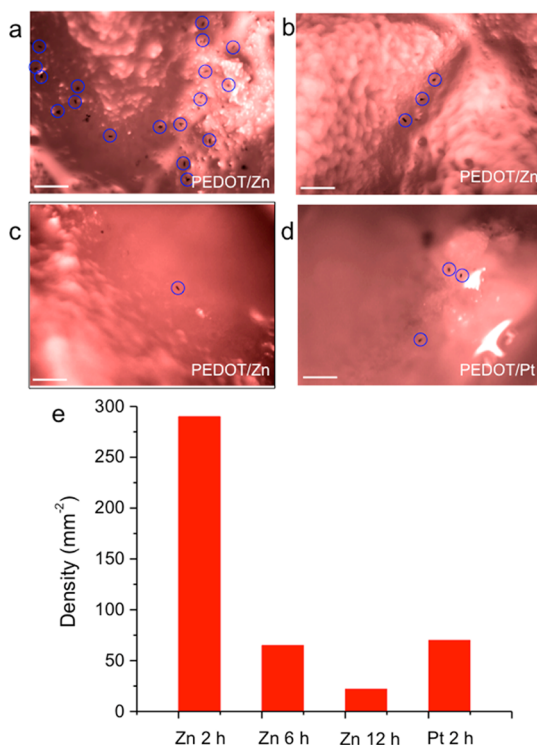


Figure 2. Tissue retention of PEDOT/Zn micromotors. (a–d) Microscopic images illustrate the retained micromotors on the stomach tissues collected at (a) 2 h, (b) 6 h, and (c) 12 h post-oral administration of PEDOT/Zn micromotors and (d) 2 h post-oral administration of PEDOT/Pt micromotors (serving as a negative control). Scale bars, 100 μm . (e) Enumeration of the density of PEDOT/Zn and PEDOT/Pt micromotors retained on the stomach tissues at the different times after the administration.

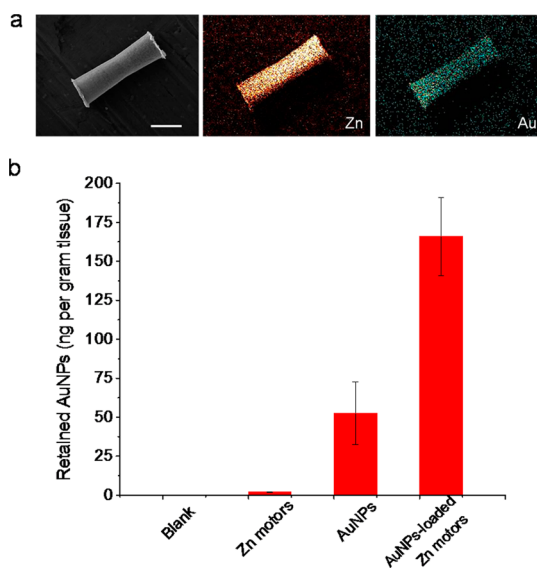


Figure 3. *In vivo* cargo delivery. (a) SEM image of a AuNP-loaded PEDOT/Zn micromotor (left) and EDX analysis illustrating the presence of Zn (middle) and Au (right) within the motor. Scale bar, 5 μ m. (b) Inductively coupled plasma-mass spectrometry (ICP-MS) analysis of the amount of gold retained on the stomach tissues. The AuNP-loaded PEDOT/Zn micromotors or AuNPs were administered orally to the mice, and the stomach tissues were collected 2 h post the administration.

PEDOT/Zn micromotors in gastric acid at physiological temperature (37 °C). No obvious difference in the propulsion behavior was observed between regular and AuNPs-loaded micromotors. Oral administration of these AuNPs-loaded PEDOT/Zn micromotors into the mouse stomach led to their movement in the gastric fluid and binding to the mucus layer on the stomach wall. The zinc dissolution under the gastric acidic conditions is accompanied by autonomous release and delivery of the encapsulated AuNPs cargo to the stomach tissue during this *in vivo* operation. The motor-based active delivery strategy resulted in distinct improvement in the delivery efficiency compared to the common passive diffusion of orally administered AuNPs. The amount of the released AuNPs retained on the mouse stomach was quantified by inductively coupled plasma/mass spectrometry (ICP-MS). As shown in Figure 3b, this spectroscopic metal analysis demonstrates that under the same experimental conditions the mice treated orally with AuNPs alone retained 53.6 ng Au per gram tissue compared to 168 ng Au per gram tissue for the mice treated with PEDOT/Zn micromotors loaded with an equivalent amount of AuNPs. Regular PEDOT/Zn micromotors, without AuNPs loading, were used as the control. Apparently, loading the AuNPs cargo onto the self-propelled “mother ship” micromotor leads to a significantly (>3-fold) larger retention of AuNPs on the stomach tissue compared to the orally administrated NPs. The high retention of AuNPs can be attributed to the effective penetration and retention of the

micromotors that will concentrate and localize the AuNP payloads on the stomach wall. Moreover, the subsequent self-dissolution of the Zn-based motors will release the AuNPs to the mucus layer, which will further trap and retain the released AuNPs. These findings clearly illustrate the importance of the micro-motor propulsion for enhancing the delivery efficiency compared to the common passive diffusion. While the concept of *in vivo* cargo delivery of PEDOT/Zn micromotors was illustrated through the loading of model AuNPs, it could be readily expanded to the simultaneous encapsulation and rapid delivery of a wide variety of payloads possessing different functions such as therapy, diagnostics, and imaging. Unlike most existing micromotors, Zn-based micromotors destroy themselves upon completing their cargo delivery mission.²⁰ It is also possible to add additional functionalities to these micromotors through bulk or surface modifications^{14,15,19,20,24–26} toward diverse biomedical applications.

Finally, we evaluated the acute toxicity of the biodegradable micromotors on healthy mice. Toxicity is a primary issue in any live animal experiment and hence in practical real-world *in vivo* applications of micromotors. The main degradation product of the present micromotors is Zn²⁺, which is an essential multipurpose nutrient involved in many aspects of metabolism and found in all body tissues.²⁷ In the study, mice were orally administered with PEDOT/Zn micromotors, AuNPs-loaded PEDOT/Zn micromotors, free AuNPs, or PBS. Mice were fasted overnight before administrating these samples to avoid the influence of food in the digestive tracts. All the mice were sacrificed 6 h after administrating the micromotors or the AuNPs. The longitudinal sections of gastric tissues obtained from mice were collected and rinsed three times with PBS. The tissue sections were stained with hematoxylin and eosin (H&E). The gastric tissue treated with PEDOT/Zn micromotors maintained an intact structure with a clear layer of epithelial cells (Figure 4c), which was similar to the gastric samples treated with PBS (Figure 4a). The gastric tissue treated with free AuNPs (Figure 4e) and with AuNPs-loaded PEDOT/Zn micromotors (Figure 4g) showed no apparent toxicity as well. The potential toxicity of the PEDOT/Zn micromotors was further evaluated using gastric tissue sections by a terminal deoxynucleotidyl transferase-mediated deoxyuridine triphosphate nick-end labeling (TUNEL) assay to examine the level of gastric epithelial apoptosis as an indicator of gastric mucosal homeostasis.²⁸ No apparent increase in gastric epithelial apoptosis was observed for treatment groups involving PEDOT/Zn micromotors (Figure 4d), free AuNPs (Figure 4f), and AuNPs-loaded PEDOT/Zn micromotors (Figure 4h), compared to the PBS control group (Figure 4b). The absence of any detectable gastric histopathologic change and toxicity indicates that the orally administrated

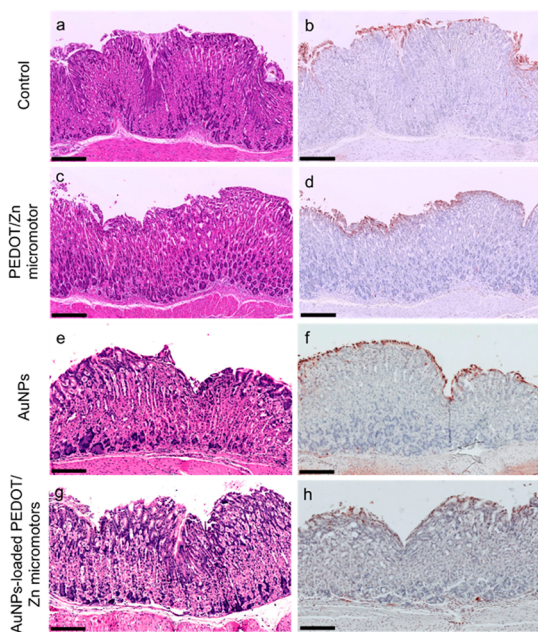


Figure 4. Toxicity evaluation of PEDOT/Zn micromotors. The mouse stomach was treated with PBS buffer (a, b), PEDOT/Zn micromotor (c, d), AuNPs (e, f), and AuNP-loaded PEDOT/Zn micromotors (g, h). At 6 h post-treatment, the mice were sacrificed and sections of the mouse stomach were processed as described in the Methods section and stained with H&E assay (a, c, e, and g) or TUNEL assay (b, d, f, and h). Scale bars, 250 μm .

PEDOT/Zn micromotors and AuNPs-loaded PEDOT/Zn micromotors are safe for the model mouse. While these Zn-based micromotors can penetrate the mucus layer on the stomach wall and thus improve the retention of the motors in the mouse's stomach, such penetration and retention do not induce a destructive effect on the gastric epithelial cells. The PEDOT polymer is a known noncytotoxic material which shows no apparent immunological response.²⁹ Similarly, zinc is a biocompatible

"green" nutrient trace element, vital for numerous body functions and processes. Accordingly, the PEDOT/Zn micromotors leave no harmful products following their movement, cargo delivery, and self-destruction in the stomach fluid, making them attractive nanoshuttles in living organisms. The absence of toxic effects in the stomach is in agreement with the *in vitro* study of the influence of micromotors on cell viability.¹⁸ It should be pointed out that changing the micromotor composition would require reassessment of the toxic response.

CONCLUSION

We reported the first *in vivo* study of artificial micro-motors using a live mouse model and characterized their distribution, retention, cargo delivery, and toxicity profile in mouse stomach. These acid-powered micromotors were applied to the stomach of living mice through gavage administration, and their retention on the gastric tissue was investigated, along with a related toxicity profile. The self-propulsion in the local stomach environment led to greatly improved tissue penetration and retention. Autonomous and efficient *in vivo* release and delivery of cargo payloads upon the self-destruction of the motors were also demonstrated. Such an active motor-based delivery strategy offers dramatic improvement in the efficiency compared to the common passive diffusion of orally administrated cargoes. While additional *in vivo* characterizations are warranted to further evaluate the performance and functionalities of various man-made micromotors in living organisms, this study represents the very first step toward such a goal. Our new findings and insights are thus expected to advance the field of synthetic nano/micromotors and to promote interdisciplinary collaborations toward expanding the horizon of man-made nanomachines in medicine.

METHODS

Synthesis of Zn-Based Micromotors. The PEDOT/Zn micromotors were prepared using a template-directed electrodeposition protocol.^{19,21} The Cyclopore polycarbonate membranes, containing a 5 μm diameter (Catalog No. 7060-2513; Whatman, Maidstone, U.K.) conical-shaped micropores, were employed as the templates. A 75 nm thick gold film was first sputtered on one side of the porous membrane to serve as the working electrode using the Denton Discovery 18. Sputtering was performed at room temperature for 90 s under a vacuum of 5×10^{-6} Torr, DC power 200 W, Ar flow of 3.1 mT, and rotation speed of 65 rpm. A Pt wire and a Ag/AgCl electrode (with 3 M KCl) were used as counter and reference electrodes, respectively. The membrane was then assembled in a plating cell with an aluminum foil serving as a contact. First, the outer PEDOT layer of the microtubes was prepared by electropolymerization at +0.80 V using a charge of 0.06 C from a plating solution containing 15 mM EDOT, 7.5 mM KNO_3 , and 100 mM sodium dodecyl sulfate (SDS). Subsequently, the inner zinc tube was deposited galvanostatically at -6 mA for 1 h from a commercial zinc plating solution containing 80 g L⁻¹ ZnSO_4 and 20 g L⁻¹ H_3BO_3 (buffered to pH = 2.5 with sulfuric acid). For the PEDOT/Pt control micromotors,

the inner Pt tube was deposited galvanostatically at -2 mA for 10 min from a commercial platinum plating solution (Platinum RTP; Technic Inc., Anaheim, CA). The sputtered gold layer was removed by hand polishing with a 3–4 μm alumina slurry. The membrane was then dissolved in methylene chloride for 10 min to completely release the microtubes. The microtubes were collected by centrifugation at 6000 rpm for 3 min and washed repeatedly with methylene chloride, followed by ethanol and ultrapure water (18.2 M Ω ·cm), three times each. Finally, the microtubes from the whole piece of membrane were dispersed into 1.2 mL of ultrapure water. The simulated gastric acid (pH 1.2) was prepared by adding 2.0 g NaCl and 7 mL of HCl (12 M) in 1.0 L of ultrapure water (18.2 M Ω ·cm).

Stomach Retention of PEDOT/Zn Micromotors. To measure the retention of the PEDOT/Zn micromotors, ICR male mice at 6 weeks of age were randomly assigned to 4 groups ($n = 3$) and orally administered with 0.3 mL of the PEDOT/Zn micromotor or PEDOT/Pt micromotor solution by oral-gavage. Mice were sacrificed at 2, 6, or 12 h post-administration of PEDOT/Zn micromotors and 2 h post-administration of PEDOT/Pt micromotors, and their stomachs were removed from the abdominal cavity. The stomachs were cut open along the greater curvature, the gastric content was removed, and the gastric

fluid containing excess micromotors was washed away. The micromotors retained on the stomach lining of the mice from each group were counted under an optical microscope.

Cargo Delivery by PEDOT/Zn Micromotors. To study the capability of PEDOT/Zn micromotors as a carrier for cargo delivery, AuNPs were chosen as a model payload. AuNPs were prepared as previously described.³⁰ Briefly, a sodium citrate solution (2.2 mM) was dissolved into DI water (150 mL) in a three-neck round-bottom flask and heated to 100 °C, followed by addition of a HAuCl₄ aqueous solution (1.0 mL, 25 mM). The reaction mixture was maintained at the boiling temperature for an additional 3.5 min followed by cooling to room temperature. The resulting AuNPs (20 mL) were poured into HAuCl₄ (8 mL, 2.5 mM, 0.008g) under magnetic stirring. Then, a freshly prepared NH₂OH solution (40 mg in 4 mL) was added dropwise and stirred for 30 min to allow the reduction of HAuCl₄ to form AuNPs with diameters of 50 nm. The particle size (diameter, nm) was measured by DLS on a Zetasizer Nano ZS (model ZEN3600 from Malvern Instruments). To prepare the AuNPs-loaded micromotors, the PEDOT outer layer was electropolymerized first in the 5 μm diameter membrane template at +0.80 V using a charge of 0.06 C from a plating solution containing 15 mM EDOT, 7.5 mM KNO₃, and 100 mM sodium dodecyl sulfate (SDS). Then, AuNPs were loaded into the membranes by the encapsulation method. Solutions of AuNPs were passed through membrane pores by vacuum infiltration before the zinc deposition. A polycarbonate membrane with pore sizes of 15 nm was placed below the sputtered Au film of the membrane containing PEDOT microtubes to retain the AuNPs within the upper 5 μm membrane pores. The membrane was then assembled in a plating cell for electrodeposition of zinc.

For the *in vivo* cargo delivery experiments, ICR male mice at 6 weeks of age were randomly assigned to three groups (*n* = 4) to receive free AuNPs, AuNPs-loaded PEDOT/Zn micromotors, and regular PEDOT/Zn micromotors as the control. Each mouse in the first two groups was administered orally (by oral-gavage) 0.3 mL of the free AuNPs solution, and of the AuNPs-loaded PEDOT/Zn micromotors containing the same amount of AuNPs. After 2 h of administration, the mice were sacrificed and the stomach was removed from the abdominal cavity. The stomach was cut along the greater curvature and rinsed with PBS. Gastric tissue of the mouse from each group was weighted. The tissue was added to 3 mL of aqua regia consisting of concentrated nitric acid and hydrochloric acid (Sigma-Aldrich, trace element analysis grade) in a volume ratio of 1:3. The mixture was left at room temperature for 12 h, followed by annealing at 80 °C for 6 h to remove the acids. The sample was then resuspended with 3 mL of DI water. Inductively-Coupled Plasma Mass-Spectrometry (ICP-MS) was used to quantify the amount of AuNPs delivered and retained in the stomach tissue.

In Vivo Toxicity Study. To evaluate the toxicity of PEDOT/Zn micromotors *in vivo*, ICR male mice at 6 weeks of age were orally administered with 0.3 mL of the PEDOT/Zn micromotors, as well as with free AuNPs or AuNPs-loaded PEDOT/Zn micromotors. Mice administered with PBS were used as a negative control. At 6 h after the administration, the mice were sacrificed and the stomachs were collected for histological analysis. The longitudinal sections of the gastric tissue were fixed in neutral-buffered 10% formalin and then embedded in paraffin. The tissue sections were stained with hematoxylin and eosin (H&E). Epithelial cell apoptosis was evaluated by the terminal deoxynucleotidyl transferase-mediated deoxyuridine triphosphate nick-end labeling (TUNEL) assay (Boehringer Mannheim, Indianapolis, IN). Sections were visualized by the Hamamatsu NanoZoomer 2.0HT, and the images were processed using NDP viewing software. All animal experiments were in compliance with institutional animal use and care regulations.

Equipment. Template electrochemical deposition of micromotors was carried out with a CHI 661D potentiostat (CH Instruments, Austin, TX). SEM images were obtained with a Phillips XL30 ESEM instrument, using an acceleration potential of 20 kV. The SEM images were taken using fresh micromotor samples. Mapping elemental analysis was carried out using an Oxford EDX attached to the SEM instrument and operated by Inca software. Microscope images and videos were captured by

an inverted optical microscope (Nikon Instrument Inc. Ti-S/L100), coupled with a 10× objective, using Hamamatsu digital camera C11440 along with the NIS-Elements AR 3.2 software. The propulsion experiments under physiological temperature were carried out using a Peltier - thermoelectric cooler module (CH-109-1.4-1.5) coupled with a K type thermocouple and a dual digital display PID temperature controller SSR. The size of the gold particle (diameter, nm) was measured by DLS on a Zetasizer Nano ZS (model ZEN3600 from Malvern Instruments). The amount of the released AuNPs retained on the mouse stomach was quantified using an ICP-MS analyzer (PerkinElmer Optima 3000 DV).

Conflict of Interest: The authors declare no competing financial interest.

Supporting Information Available: Supporting methods and videos. This material is available free of charge via the Internet at <http://pubs.acs.org>.

Acknowledgment. This project received support from the Defense Threat Reduction Agency-Joint Science and Technology Office for Chemical and Biological Defense (Grant Nos. HDTRA1-14-1-0064 and HDTRA1-13-1-0002) and from the National Institute of Diabetes and Digestive and Kidney Diseases of the National Institutes of Health (Award Number R01DK095168). W.G. is a HHMI International Student Research fellow. R.D. acknowledges the China Scholarship Council (CSC) for the financial support. We thank Michael Galarnyk and Zhiguang Wu for their assistance.

REFERENCES AND NOTES

- Mallouk, T. E.; Sen, A. Powering Nanorobots. *Sci. Am.* **2009**, *300*, 72–77.
- Mirkovic, T.; Zacharia, N. S.; Scholes, G. D.; Ozin, G. A. Fuel for Thought: Chemically Powered Nanomotors Out-Swim Nature's Flagellated Bacteria. *ACS Nano* **2010**, *4*, 1782–1789.
- Wang, J. *Nanomachines: Fundamentals and Applications*; Wiley-VCH: Weinheim, Germany, 2013.
- Mei, Y. F.; Solovev, A. A.; Sanchez, S.; Schmidt, O. G. Rolled-up Nanotech on Polymers: From Basic Perception to Self-Propelled Catalytic Microengines. *Chem. Soc. Rev.* **2011**, *40*, 2109–2119.
- Paxton, W. F.; Kistler, K. C.; Olmeda, C. C.; Sen, A.; St. Angelo, S. K.; Cao, Y.; Mallouk, T. E.; Lammert, P. E.; Crespi, V. H. Catalytic Nanomotors: Autonomous Movement of Striped Nanorods. *J. Am. Chem. Soc.* **2004**, *126*, 13424–13431.
- Guix, M.; Mayorga-Martinez, C. C.; Merkoci, A. Nano/Micromotors in (Bio) chemical Science Applications. *Chem. Rev.* **2014**, *114*, 6285–6322.
- Wilson, D. A.; Nolte, R. J. M.; van Hest, J. C. M. Autonomous Movement of Platinum-Loaded Stomatocytes. *Nat. Chem.* **2012**, *4*, 268–274.
- Loget, G.; Kuhn, A. Electric Field-Induced Chemical Locomotion of Conducting Objects. *Nat. Commun.* **2011**, *2*, 535.
- Wang, J.; Gao, W. Nano/Microscale Motors: Biomedical Opportunities and Challenges. *ACS Nano* **2012**, *6*, 5745–5751.
- Nelson, B. J.; Kaliakatsos, I. K.; Abbott, J. J. Microrobots for Minimally Invasive Medicine. *Annu. Rev. Biomed. Eng.* **2010**, *12*, 55–85.
- Solovev, A. A.; Xi, W.; Gracias, D. H.; Harazim, S. M.; Deneke, C.; Sanchez, S.; Schmidt, O. G. Self-Propelled Nanotools. *ACS Nano* **2012**, *6*, 1751–1756.
- Mei, Y. F.; Huang, G. S.; Solovev, A. A.; Urena, E. B.; Monch, I.; Ding, F.; Reindl, T.; Fu, R. K. Y.; Chu, P. K.; Schmidt, O. G. Versatile Approach for Integrative and Functionalized Tubes by Strain Engineering of Nanomembranes on Polymers. *Adv. Mater.* **2008**, *20*, 4085–4090.
- Wu, Z.; Wu, Y.; He, W.; Lin, X.; Sun, J.; He, Q. Self-Propelled Polymer-Based Multilayer Nanorockets for Transportation and Drug Release. *Angew. Chem., Int. Ed.* **2013**, *52*, 7000–7003.

14. Balasubramanian, S.; Kagan, D.; Hu, C. J.; Campuzano, S.; Lobo-Castaño, M. J.; Lim, N.; Kang, D. Y.; Zimmerman, M.; Zhang, L.; Wang, J. Micromachine-Enabled Capture and Isolation of Cancer Cells in Complex Media. *Angew. Chem., Int. Ed.* **2011**, *50*, 4161–4164.
15. Campuzano, S.; Orozco, J.; Kagan, D.; Guix, M.; Gao, W.; Sattayasamitsathit, S.; Claussen, J. C.; Merkoci, A.; Wang, J. Bacterial Isolation by Lectin-Modified Microengines. *Nano Lett.* **2012**, *12*, 396–401.
16. Wang, W.; Li, S.; Mair, L.; Ahmed, S.; Huang, T. J.; Mallouk, T. E. Acoustic Propulsion of Nanorod Motors Inside Living Cells. *Angew. Chem., Int. Ed.* **2014**, *126*, 3265–3268.
17. Mhana, R.; Qiu, F.; Zhang, L.; Ding, Y.; Sugihara, K.; Zenobi-Wong, M.; Nelson, B. J. Artificial Bacterial Flagella for Remote-Controlled Targeted Single-Cell Drug Delivery. *Small* **2014**, *10*, 1953–1957.
18. Chng, E. L. K.; Zhao, G.; Pumera, M. Towards Biocompatible Nano/Microscale Machines: Self-Propelled Catalytic Nanomotors Not Exhibiting Acute Toxicity. *Nanoscale* **2014**, *6*, 2119–2124.
19. Gao, W.; Uygun, A.; Wang, J. Hydrogen-Bubble-Propelled Zinc-Based Microrockets in Strongly Acidic Media. *J. Am. Chem. Soc.* **2012**, *134*, 897–900.
20. Sattayasamitsathit, S.; Kou, H.; Gao, W.; Thavarajah, W.; Kaufmann, K.; Zhang, L.; Wang, J. Fully Loaded Micro-motors for Combinatorial Delivery and Autonomous Release of Cargoes. *Small* **2014**, *10*, 2830–2833.
21. Gao, W.; Sattayasamitsathit, S.; Uygun, A.; Pei, A.; Ponedal, A.; Wang, J. Polymer-Based Tubular Microbots: Role of Composition and Preparation. *Nanoscale* **2012**, *4*, 2447–2453.
22. Lai, S. K.; Wang, Y. Y.; Hanes, J. Mucus-Penetrating Nanoparticles for Drug and Gene Delivery to Mucosal Tissues. *Adv. Drug Delivery Rev.* **2009**, *61*, 158–171.
23. Daniel, M. C.; Astruc, D. Gold Nanoparticles: Assembly, Supramolecular Chemistry, Quantum-Size-Related Properties, and Applications toward Biology, Catalysis, and Nanotechnology. *Chem. Rev.* **2004**, *104*, 293–346.
24. Kuralay, F.; Sattayasamitsathit, S.; Gao, W.; Uygun, A.; Katzenberg, A.; Wang, J. Self-Propelled Carbohydrate-Sensitive Microtransporters with Built-In Boronic Acid Recognition for Isolating Sugars and Cells. *J. Am. Chem. Soc.* **2012**, *134*, 15217–15220.
25. Orozco, J.; Cortes, A.; Cheng, G.; Sattayasamitsathit, S.; Gao, W.; Feng, X.; Shen, Y.; Wang, J. Molecularly Imprinted Polymer-Based Catalytic Micromotors for Selective Protein Transport. *J. Am. Chem. Soc.* **2013**, *135*, 5336–5339.
26. Zhao, G.; Wang, H.; Sanchez, S.; Schmidt, O. G.; Pumera, M. Artificial Micro-Cinderella Based on Self-Propelled Micromagnets for the Active Separation of Paramagnetic Particles. *Chem. Commun.* **2013**, *49*, 5147–5149.
27. King, J. C. Zinc: An Essential but Elusive Nutrient. *Am. J. Clin. Nutr.* **2011**, *94*, 6795–6845.
28. Que, F. G.; Gores, G. J. Cell Death by Apoptosis: Basic Concepts and Disease Relevance for the Gastroenterologist. *Gastroenterology* **1996**, *110*, 1238–1243.
29. Asplund, M. Toxicity Evaluation of PEDOT/Biomolecular Composites Intended for Neural Communication Electrodes. *Biomed. Mater.* **2009**, *4*, 045009.
30. Ji, T.; Lirtsman, V. G.; Avny, Y.; Davidov, D. Preparation, Characterization, and Application of Au-Shell/Polystyrene Beads and Au-Shell/Magnetic Beads. *Adv. Mater.* **2001**, *13*, 1253–1256.